

# **Geo-Environmental Assessment of the Suez Canal Area, using Remote sensing and GIS Techniques**

**S.Ahmed<sup>1</sup> and M.F. Kaiser<sup>2</sup>**

## **Abstract**

The Impacts of geologic, topographic and hydrologic characters on the thermal environment was assessed in the Ismailia-Bitter Lakes area. Digital Elevation Model extracted from the SRTM data shows that the waterlogged areas are distributed at low topographic localities. The drainage pattern extracted from the ETM+ image data and SRTM (DEM) using ArcGIS techniques show that all tributaries are accumulated toward the waterlogging localities. Image classification identified five land use categories at the concerned site, including surface water, sand cover, limestone, salt crust and Nile deposits & cultivated areas. Surface water were outlined and measured during 1987-2012; its surface areas increase from 56 km<sup>2</sup> in year 1987 to 150 km<sup>2</sup> in year 2012 with a rate of 3.8 km<sup>2</sup>/year. Thermal bands were processed to obtain radiant surface temperatures to investigate spatial and temporal Urban Heat Island effects associated with increasing waterlogged areas. Land Surface Temperature (LST) decreases from very high in year 1987 to moderate and low in year 2012. This study provides useful information for understanding the relationship between the expansion of surface water and land surface temperature.

**Keywords:** Urban Heat Island, Land use/Land cover changes, water logging, Image classification, Ismailia-Bitter lakes area.

## **1 Introduction**

Water logging is the most serious and extensive environmental problem that forms soil salinization and land degradation in Ismailia-Bitter lakes area. The Suez Canal zone is occupied by Quaternary deposits which consist of friable and loose sand sheets. The sand grains are mainly quartz with occasional contamination of carbonate grains in some localities [1]. [2] and [3] studied the shallow sediments of the El Timsah and Bitter Lakes and concluded that, these shallow sediments are mainly sands, silt and clay with presence of some gypsum lenses. The sediments are fluvio-marine origin characterized by the

---

<sup>1</sup>Department of Physics, AL-Arish Suez Canal University

<sup>2</sup>Department of Geology, Suez Canal University, Egypt

presence of Nilotic minerals. Flood silt sheets cover most of the study area, it is mainly composed of muddy and silty sand varying in thickness between 0.5 and 6 m [4]. Ismailia-Bitter lakes area is located between longitudes  $32^{\circ} 15'$  and  $32^{\circ} 35'$  E and Latitudes  $30^{\circ} 10'$  and  $30^{\circ} 37'$  N, it occupies about  $2000\text{km}^2$  along the Suez Canal zone (Fig. 1). It is one of the most important areas, in Egypt, for future agricultural and agro-industrial development. The underflow and agricultural drainage water are draining upward towards the low wetlands and surface water. This research aims at to analyze and understand the local changes in thermal environment that occur during 1987-2012 in Ismailia-Bitter Lakes area. The concerned site has been experiencing a rapid expansion in waterlogged area over the last 25 years.

## 2 Field Observation and Soil Description

Field study was undertaken to describe the land cover and soils characteristics at the concerned sites and measure 15 ground control points to check the accuracy of the image to map registration and to get image supervised classification. Two main landscapes are recorded by [5] in the Suez Canal district, including fluvio-marine flats in the north and the river terraces, fluvial and deltaic origin, in the south. Many sub-landscapes and a transitional zone, strongly subjected to wind activities, are observed between the two main landscapes.

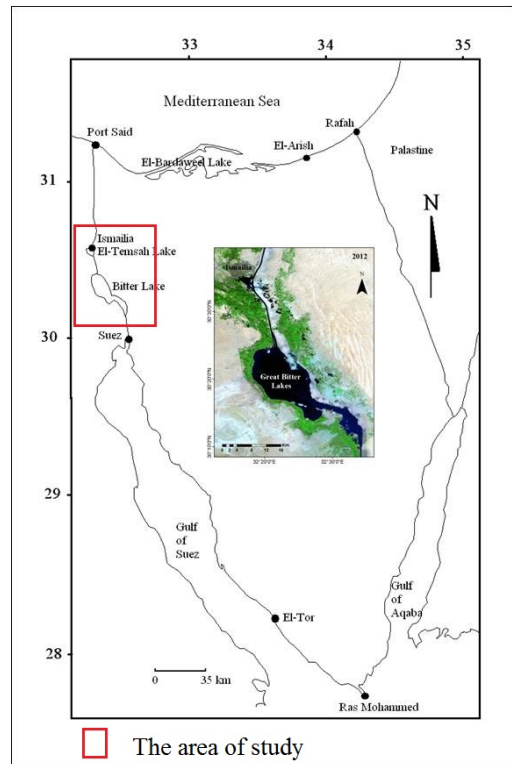


Figure 1: The area of study

The transitional zone consists of nearly flat gypsum swamps and gypsiferous sand soils, windblown sand soils and a small strip of transitional soil, which is either sand covered with clay or clay covered by sand. During the field visits, it was noticed that the area of study is covered by cultivated lands besides three soil types including; shifting sand dunes, gypsiferous sand, fluvial soils.

Characteristics of these soils are recognized as follows:

### **2.1 Shifting Sand Dunes Soils**

This type of soil has local origin, which is mainly composed of coarse wind-blown sand without clay and silt. The transition zone between the terraces and fluvio-marine deposits are characterized by dunes, which most of them are still active.

### **2.2 Gypsiferous Deposits**

This sediment deposited in recent stage and observed in low, swampy and flooded areas. It is mainly composed of pure gypsum, gypsiferous clay or gypsiferous sand.

### **2.3 Fluvial Soils**

These deposits have fluvial origin, during Pleistocene age, with elevation reach to 30-50m height, above the present river level. They consist of flat gravelly, loamy and partly fine-sandy to silty material strongly subjected to wind and water erosion. Environmental conditions along the Suez Canal coastal zone and associated lakes will be subjected rapid changes in the next decades [6]. The changes will be particularly in the soil nature due to the increase of evaporation, the decrease in fresh-water supply following the future expansion of land reclamation on both sides of the canal.

## **3 Methods and Techniques**

Remote sensing and geographic information system techniques are considered as powerful and effective tools and are widely applied in detecting the spatio-temporal dynamics of land use cover changes [7]. The LST is derived from satellite thermal infrared (TIR) imagery [8]. Two sets of remote sensing data are used to conduct this research including Landsat5 Thematic Mapper (TM) in 1987 and Enhanced Landsat Thematic Mapper Images Plus (ETM+) in year 2012. In this research, remote sensing image processing and Geographic Information Systems techniques were utilized to classify land cover and extract urban heat island in the Suez Canal area during 1987-2012. The procedure will be discussed as follows:

### **3.1 Image Enhancement**

Commonly used image processing techniques include image classification, change detection and extraction of topographic features. These are all used to extract useful information that assists in image interpretation. Two sets of remote sensing data are acquired in this study aiming to detect, outline and monitor surface water in Ismailia-

Bitter Lakes area. Remote Sensing and GIS techniques can be extremely useful in accurate mapping and quantification of waterlogged area and salt-affected soils. The possible forms of digital image manipulation are literally infinite. However, in this research these procedures can be categorized into the following types of computer-assisted operations: images classification and change detection.

### **3.1.1 Image classification**

The intent of the classification process is to categorize all pixels in a digital image into one of several land cover classes, or "themes". This categorized data may then be used to produce thematic maps of the land cover present in an image. Normally, multispectral data are used to perform the classification and, indeed, the spectral pattern present within the data for each pixel is used as the numerical basis for categorization [9]. The objective of image classification is to identify and portray, as a unique gray level (or color), the features occurring in an image in terms of the object or type of land cover these features actually represent on the ground. Image classification is perhaps the most important part of digital image analysis. It is very nice to have a "pretty picture" or an image, showing a magnitude of colors illustrating various features of the underlying terrain, but it is quite useless unless to know what the colors mean. Two main classification methods are Supervised Classification and Unsupervised Classification. With unsupervised classification, however, clustering software is used to uncover the commonly occurring landcover types, with the analyst providing interpretations of those cover types at a later stage [10]. Unsupervised classification was carried out on the two data sets of the images separately using a histogram peak cluster technique to identify dense areas or frequently occurring pixels [11]; [12]; [13]. To undertake supervised classification, it is necessary to collect training samples that relate ground cover to spectral signatures for a given geographic location. All spectral classes in the scene were represented in the various subareas. These areas were then clustered independently and the spectral classes from the various areas were analyzed to determine their identity. Clusters representing land cover types that were similar were combined [13].

### **3.1.2 Change detection**

Change detection is the process of identifying differences in the state of an object or phenomenon by observing it at different times [14]. Timely and accurate change detection of earth's surface features provides the foundation for better understanding relationships and interactions between human and natural phenomena to better manage and use resources. Change detection techniques was used in this study to monitor the changes in the areas of surface water during 1987-2012.

### **3.1.3 DEM and topographic map**

The SRTM was a National Aeronautics and Space Administration (NASA) mission conducted in 2000 to obtain elevation data for most of the world, generating the most complete high-resolution digital topographic database for Earth. It is the current dataset of choice for DEM production because it has a fairly high resolution (w90 m at the equator, <30 m in the US). Three resolution outputs are available: 1-km and 90-m resolutions for the world and 30-m resolution for the US. SRTM digital elevation data, originally produced by NASA, represent a major breakthrough in global digital mapping and a

major advance in the accessibility of high-quality elevation data for large portions of the tropics and other areas of the developing world. The hydrogeology tools in ArcGIS provide a method to describe the physical characteristics of a surface using a DEM as input.

### 3.2 Calculation of Urban Heat Island (UHI)

ENVI 4.8 and ERDAS Imagine 9.3 were utilized to retrieve UHI of the study area. Landsat calibration equation of [15] was used to convert the digital number (DN) of the Landsat TM/ETM+ thermal infrared (TIR) band (10.44–12.42  $\mu\text{m}$ ) to the spectral radiance in unit ( $\text{W m}^{-2} \mu\text{m}^{-1} \text{sr}^{-1}$ ). All specific calibration coefficients and other related parameters including sun elevation, gain and offset were extracted from a level 1 product header or ancillary data record. The spectral radiance was converted to the at-satellite brightness temperature [15]; [16].

The land surface temperature can be extracted using equation (1), [17]; and [18]:

$$T_s = \frac{T_i}{1 + \left(\lambda \frac{T_i}{\rho}\right) \ln \varepsilon} \quad (1)$$

Where:

$T_s$ : is the land surface temperature

$T_i$ : is the effective at-satellite brightness temperature in kelvin

$\lambda$ : is the wavelength of the emitted radiance ( $\lambda = 11.5 \mu\text{m}$  for Landsat band 6 data)

$\rho = \frac{hc}{\sigma} = 1.438 \times 10^{-2} \text{mk}$ , where  $h$  is the Plank's constant ( $6.626 \times 10^{-34} \text{Js}$ ),  $c$  is the velocity of light ( $2.998 \times 10^8 \text{ m/s}$ ) and  $\sigma$  is the Boltzmann constant ( $5.67 \times 10^{-8} \text{ Wm}^{-2} \text{k}^{-4} = 1.38 \times 10^{-23} \text{ J/k}$ ).

$\varepsilon$ : is the land surface spectral emissivity

Normalized Difference Vegetation Index (NDVI) was used to transform multispectral data into a single image band representing vegetation distribution [19]. The NDVI values indicate the amount of green vegetation present in the pixel. Standard algorithm was computed using ENVI 4.8 software that uses the equation published in [20]. Higher NDVI values indicate more green vegetation, valid results fall between -1 and +1. In highly vegetated areas, the NDVI typically ranges from 0.1 to 0.6, whereas urban surface and water values are negative. Normalization method used to extract Urban Heat Island (UHI) from Land Surface Temperature (LST), (Equation, 2).

$$U_i = \frac{T_s - T_{\min}}{T_{\max} - T_{\min}} \quad (2)$$

Where:

$U_i$ : is the Urban Heat Island

$T_s$ : is the Land Surface Temperature

$T_{\min}$  and  $T_{\max}$ : are the minimum and maximum LST retrieved from all data sets with excluding of extremes.

## 4 Results Discussion

Monitoring and analysis of the recent landcover dynamics through the integration of remote sensing and GIS could provide base information for documenting water logging trends. Two satellite images taken over a span of 25 years (1987–2012) coupled with a 30-m DEM and field observations served as the basic sources of data. Image classifications and change detection techniques were applied to determine changes between the available images. Unsupervised/ supervised classification was employed to obtain a detailed land use classification data. The classes in the unsupervised classification scheme were very similar to those produced in the supervised classification. Maximum likelihood supervised classification was applied to Landsat images acquired in 1987 and 2012 for the assessment of land cover classes. Five land use categories were identified, including surface water, sand cover, limestone, salt crust and Nile deposits & cultivated areas (Fig. 2). Each class was verified in the field using a Garmin 38 GPS unit; more than 25 ground data sites were visited and checked. The results confirmed an acceleration in the rate of water logged areas during 1987-2012. The surface water areas increased from 56 km<sup>2</sup> in 1987 to 150 km<sup>2</sup> in 2012. The non-manageable agricultural expansion, excess irrigation water and deficiency of a drainage system are the most important factors producing water logging phenomena. The seepage from the Suez Canal beds and distributaries contribute significantly to the waterlogging and subsequent salinization problem. Remote sensing and GIS result indicate that there are some factors affect the area of study and produce waterlogging problem, including 1) topography and surface elevation, 2) drainage pattern and water flow direction.

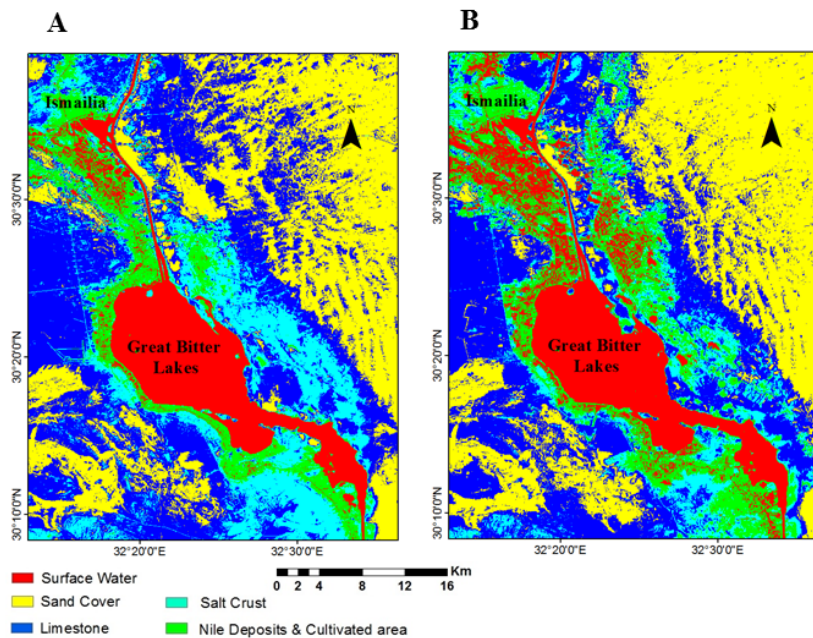


Figure 2: Monitoring of the surface water areas during 1987-2012

Digital Elevation Model extracted from the SRTM data shows that the waterlogged areas are distributed at low topographic localities (Fig. 3). The area having a low lying

topography has numerous topographic depressions which are poorly drained topographically and remain waterlogged throughout the year. The drainage pattern extracted from the ETM+ image data and SRTM (DEM) using ArcGIS techniques show that all tributaries are accumulated toward the waterlogging localities. This indicate that during the intensive rain fall, all surface and subsurface water are going along these tributaries and accumulate water at the low topographic areas and producing waterlogging problems.

In addition, remote sensing technology was used to monitor the impacts of surface water on thermal environment during 1987-2012. This was conducted through analyzing thermal infrared. Thermal bands were processed to obtain radiant surface temperatures for investigating the urban heat island effect associated with increasing surface water, both spatially and temporally (Fig. 4). Land Surface Temperature (LST) decreases from very high in year 1987 to moderate and low in year 2012.

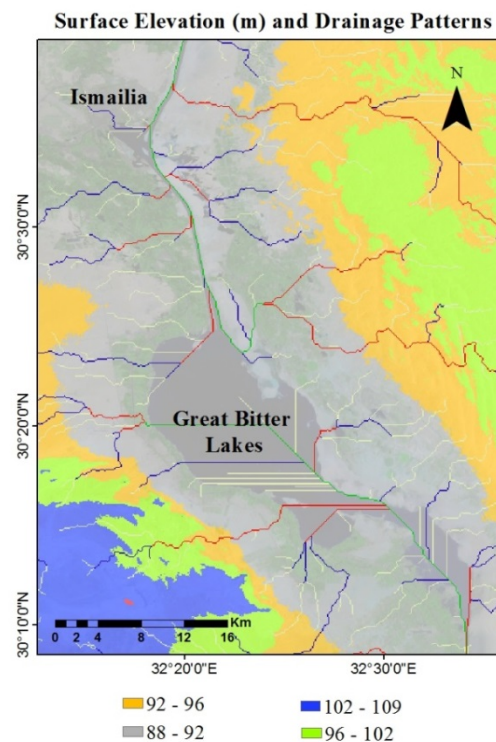


Figure 3: Surface elevation and drainage patterns in the study site

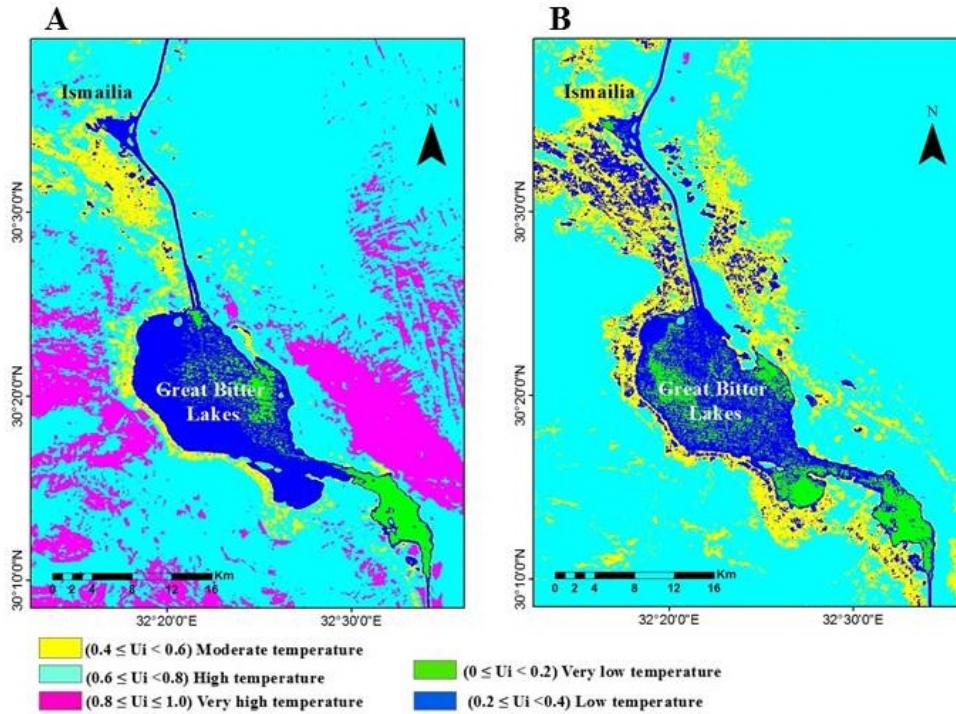


Figure 4: Urban Heat Island (UHI) range and its classification

## 5 Conclusion

Image classifications and change detection techniques were applied to determine changes between the available images. Maximum likelihood supervised classification was applied to Landsat images acquired in 1987 and 2012 for the assessment of land cover classes. Five land use categories were identified, including surface water, sand cover, limestone, salt crust and Nile deposits & cultivated areas. Each class was verified in the field using a Garmin 38 GPS unit; more than 25 ground data sites were visited and checked. The results confirmed an acceleration in the rate of water logged areas during 1987-2012. The surface water areas increased from 56 km<sup>2</sup> in 1987 to 150 km<sup>2</sup> in 2012. Digital Elevation Model extracted from the SRTM data shows that the waterlogged areas are distributed at low topographic localities. The area having a low lying topography has numerous topographic depressions which are poorly drained topographically and remain waterlogged throughout the year. Remote sensing and GIS result indicate that there are some factors affect the area of study and the area being low lying and devoid of any natural streams soon turns up into a ponded zone. The drainage pattern extracted from the ETM+ image data and SRTM (DEM) using ArcGIS techniques show that all tributaries are accumulated toward the waterlogging localities. This indicate that during the intensive rain fall, all surface and subsurface water are going along these tributaries and accumulate water at the low topographic areas and producing waterlogging problems. Remote sensing technology was used to monitor the impacts of surface water on thermal environment during 1987-2012. Thermal bands were processed to obtain radiant surface temperatures for investigating the urban heat island effect associated with increasing surface water, both

spatially and temporally. The results show decrease from very high temperature in year 1987 to moderate temperature in year 2012.

## References

- [1] El Shazly, E. M., Abd El Hady, M. A., El Shazly, M. M., El Kassas, I. A., El Ghawaby, M. A., Salman, A. B. and Morsi, M. A., "Geology and groundwater potential studies of El Ismailia master plan study area". Remote Sensing Research project, Academy of Scientific Res. and Techno., Cairo, Egypt (1975).
- [2] El Ibiary, M. G., "Shallow subsurface geological and geophysical studies at lake El Timsah, Suez Canal area". M. Sc. Thesis, Tanta Univ., Egypt, **174** p (1981).
- [3] Ramadan, F. S., "Sedimentological studies of the bottom sediment of the Suez Canal". M.Sc. Thesis, Zagazig Univ., Egypt (1984).
- [4] Geriesh, M. H., "Hydrogeological and hydrogeochemical evaluation of groundwater resources in the Suez Canal region". Ph. D. thesis, Fac. Sci. Suez Canal University (1994).
- [5] F.A.O., "High Dam soil survey", United Arab Republic: Volume III, the semi-detailed soil survey, UNDP/FAO (1964).
- [6] United Nation Environment Program (UNEP), "Vulnerability assessment of the low-lying coastal areas, in the southern part of the Suez Canal, Suez Canal University", 205pp (1997).
- [7] Weng, Q., "Remote sensing of impervious surfaces in the urban areas: requirements, methods and trends". *Remote Sensing of Environment*, **117**, 34–49 (2012). doi:10.1016/j.rse.2011.02.030
- [8] Li, J., Song, C., Cao, L., Zhu, F., Meng, X. and Wu, J., "Impacts of landscape structure on surface urban heat islands: a case study of Shanghai, China". *Remote Sensing of Environment*, **115** (12) 3249–3263 (2011).doi:10.1016/j.rse.2011.07.008
- [9] Lillesand, T. M. and Kiefer, R. W., "Remote sensing and image interpretation". John Wiley & Sons, Inc. 750 pp (1994).
- [10] Sonka, M., Hlavac, V., Boyle, R., "Image processing, Analysis and Machine vision", Chapman & Hall, London, 555pp (1993).
- [11] Eastman, J. R., "Supervised classification in IDRISI for windows version 2, tutorial exercises". Worcester, Massachusetts: Clark University. pp. 86–94 (1997).
- [12] Mather, P. M., "Computer processing of remotely-sensing images, an introduction" (2nd ed.) Chichester: John Wiley & Sons, Inc., pp. 1–75 (1999).
- [13] Lillesand, T. M., Kiefer, R. W. and Chipman, J. W., "Remote sensing and image interpretation". John Wiley & Sons, Inc., 763 pp (2004).
- [14] Singh, A., "Digital change detection techniques using remotely-sensed data". *International Journal of Remote Sensing*, **10**, 989–1003 (1989).
- [15] Chander G. and Markham B., "Revised Landsat-5 TM radiometric calibration procedures and post calibration dynamic ranges". *IEEE Transaction on Geosciences and Remote Sensing*, **41**(11) 2674-2677 (2003).
- [16] Wu C., Wang Q., Yang Z., and Wang W., "Monitoring heated water pollution of the Da YaWan nuclear power plant using TM images". *International Journal of Remote Sensing*, **28**(5), 885-890 (2007).

- [17] Xiong Y., Huang S., Chen F., Ye H., Wang C. and Zhu C., "The impacts of rapid urbanization on the thermal environment: A remote sensing study of Guangzhou, South China". *Remote sensing*, **4**, 2033-2056 (2012).
- [18] Yue, W., Liu, y., Fan P., Ye, x. and Wu, c., "Assessing spatial pattern of urban thermal environment in Shanghai, China". *Stochastic Environmental Research and Risk Assessment*, **26**, 899–911 (2012).
- [19] Rouse, J.W., Haas, R.H., Schell, J.A. and Deering, D.W., "Monitoring vegetation systems in the Great Plains with ERTS". In *Proceedings Third Earth Resources Technology Satellite-1 Symposium*, Greenbelt, NASA SP-351, 3010–3017 (1974).
- [20] Jensen, J. R., "Introductory Digital Image Processing", Prentice-Hall, New Jersey, p. 379 (1986).